Computational Energy Science

Vol. 1, No. 3, p. 150-163, 2024

Original article

Rate transient analysis of multiple wells system producing at constant bottomhole pressures

Jing Lu[1]*, Yusheng Zhai[1], Erlong Yang[1]*

[1]*Key Lab of Enhanced Oil Recovery, Ministry of Education, Northeast Petroleum University, Heilong Jiang 163000, P. R. China*

Keywords:
Analytical model
production performance
multiple wells system rate transient analysis

Cited as:
Lu, J., Zhai, Y., Yang, E. Rate transient analysis of multiple wells system producing at constant bottomhole pressures. Computational Energy Science, 2024, 1(3): 150-163.
https://doi.org/10.46690/compes.2024.03.03

Abstract:
This paper presents rate transient analysis of multiple wells system producing at constant bottomhole pressures during boundary-dominated flow period in a closed rectangular reservoir. The proposed algorithm is based on an analytical model with numerical approximation, and production decline is predicted through a series of mathematical methods such as the Laplace transform, the Dirac Delta function, convolution, the Green's function and the superposition principle. The proposed model is validated by the Computer Modeling Group (CMG) simulation, the results show that the proposed model is accurate enough to predict the production performance of multi-well system producing under constant bottomhole pressures during boundary-dominated flow period in a closed rectangular reservoir. We conclude that at a given time, the flow rate of a well decreases as the total number of wells increases and the bottomhole pressures of adjacent wells decrease, while the total reservoir production increases as the bottomhole pressures of reservoir wells decreases. And at a given time, the greater distance between the observation well and adjacent wells, the larger the flow rate and cumulative production the observation well. In terms of the decline rate of the flow rate, it depends on the number of wells, the bottomhole pressures of adjacent wells, and the size of reservoir. The conventional models presented in the literature are mostly empirical or semi-analytical, which are not grounded in fundamental theory. Our proposed model has a solid theoretical basis, it provides a computationally efficient, accurate and convenient method for predicting transient flow rates of multiple wells producing at constant bottomhole pressures in a closed rectangular reservoir.

1. Introduction

The conventional well testing method assumes a well is producing at a constant flow rate, which is difficult to maintain for a long time. And actually, it is not uncommon that a well produces under constant bottomhole pressure. Conditions under which constant pressure is maintained include steam production into a back-pressured turbine, production in a tight reservoir (Hu et al., 2012) or open flow to the atmosphere. Rate-time decline-curve analysis is the technique most extensively used by engineers in the evaluation of well performance and production forecasting when wells are produced at constant bottomhole pressures.

In most cases, production decline analysis methods are based on the Arps empirical models (Arps, 1945). Later on, Fetkovich (1973) proposed type curves of transient flow through developing the connection between the material balance and the pseudo-steady state inflow equation. Fetkovich developed a series of new type-curves, which made the Arps empirical model effective in transient flow period. Ehlig-Economides and Ramey (1981) presented a general solution of a well under constant bottomhole pressure and practical methods to transient flow rate analysis under constant pressure. The flow rate response to a step change in producing pressure allows type-curve analysis without considering the complicated wellbore storage effect. Blasingame and Lee (1986) and Palacio and Blasingame (1993) developed production decline methods that account for variations in bottomhole flowing pressure in both transient regime and boundary-dominated

Yandy Scientific Press

*Corresponding author.
E-mail address: nepulj@nepu.edu.cn (J. Lu); 228002020116@stu.nepu.edu.cn (Y. Zhai); yangerlong@nepu.edu.cn (E. Yang).

Received July 10, 2024; revised August 17, 2024; accepted September 17, 2024; available online September 20, 2024.

flow regime. The Normalized Pressure Integral (NPI) was initially developed by Blasingame et al. (1989). The NPI provides an analysis method that is based on pressure, rather than rate, and the main purpose is to present an analysis that is similar to a well test analysis. Agarwal et al. (1998) have complied and presented new decline type-curves based upon the work of both Fetkovich and Palacio–Blasingame, utilizing the concepts of the equivalence between constant rate and constant pressure solutions.

Traditional decline methods such as Arps' rate-time relations and their variations do not work for tight or shale gas wells where fracture flow is dominant. Duong (2010) presented a new empirical model for predicting the future rate of fracture-dominated shale reservoirs. Ezabadi et al. (2017) presented an integrated workflow for production data analysis and successfully applied on different cases of highly heterogeneous conventional gas reservoirs with huge complexities. Anderson et al. (2018) showed the "health" of a producing well could be measured of in terms of how much productivity loss has occurred (or is expected to occur in the future). Jha et al. (2021) presented a mathematical analysis of how incorrect estimates of initial reservoir pressure may affect rate-transient analysis in ultra-low permeability reservoirs.

The production performance of multiple wells system has received attention in the last two decades. Valko et al. (2000) presented pseudo-steady state productivity index for multiple wells producing from a closed rectangular reservoir. Umnuayponwiwat et al. (2000) presented equations of inflow performance of multiple vertical and horizontal wells in closed systems. Marhaendrajana and Blasingame (2001) presented a solution and associated analysis methodology to evaluate single well performance behavior in a multiple wells reservoir system.

The above conventional models presented in the literature are mostly empirical and not grounded in fundamental theory. Additionally, most models are developed on the basis of constant flow rate production. Lu et al. (2018) challenged the above conventional models and provided new solutions to the transient rate equation of a vertical well producing at constant bottomhole pressure in a closed circular reservoir. Lu et al. (2019) proposed a mathematical model for production performance of multiple wells producing at constant bottomhole pressures in a rectangular reservoir, but their proposed algorithm involves double infinite summation, which has huge computation, low efficiency and low precision. The mathematical models offered by Lu et al. (2019) for multiple wells are the precursors for this work.

This paper provides a computationally efficient, accurate and convenient method for predicting transient flow rates of multiple wells producing at constant bottomhole pressures in a closed rectangular reservoir. Analytical solutions with simple procedures are given to forecast the production decline of multiple wells system, the effects of the well production starting time, the number of wells, the well location, the reservoir size, and the distance between wells on transient flow rates are studied.

2. Analytical model

2.1 Basic assumptions

The basic assumptions are shown as follows:

- The reservoir has a closed boxed drainage domain with constant thickness, porosity, and permeability. Also the porous volume is bounded by lateral, top, and bottom closed boundaries.
- Initially, the reservoir has constant pressure and it is above the bubble point pressure during the field life. The transient pressure has transmitted to lateral reservoir boundary.
- No water or gas injection into the reservoir. The multiple wells are represented by uniform line sinks in the model which are located at any place in the box-shaped reservoir.
- The fluid is a single-phase liquid, with slight compressibility, constant viscosity, and formation volume factor. Also, we neglect the effect of pressure on fluid properties and gravity forces.

2.2 Governing equation, initial and boundary conditions.

The reservoir domain is a rectangular parallelepiped with length a, width b and height h, which can be expressed below:

$$\Omega = (0,a)\times(0,b)\times(0,h) \tag{1}$$

All the wells are fully penetrating, thus we may investigate the production performance in two-dimensional space.

Assume that there are two groups of producing wells in the reservoir. The wells in the first group are produced at constant but different wellbore pressures, well i is located at $(x_{p,i}, y_{p,i})$, $i = 1,2,...,N$. Well i begins to produce at time $t_{p,i}$, and $0 \le t_{p,1} \le t_{p,2} \le ... \le t_{p,N-1} \le t_{p,N}$. The wells in the second group are produced at constant but different flow rates, well j is located at $(x_{f,j}, y_{f,j})$, $j = 1,2,...,M$. Well j begins to produce at time $t_{f,j}$, and

$$0 \le t_{f,1} \le t_{f,2} \le ... \le t_{f,M-1} \le t_{f,M}$$

We can obtain the governing equation for a multiple-wells system by superposition principle (Lee et al., 2003; Lu et al., 2019):

$$\begin{aligned}\frac{\partial^2 P}{\partial x^2}+\frac{\partial^2 P}{\partial y^2} &= \left(\frac{\phi\mu C_t}{K}\right)\frac{\partial P}{\partial t} \\ &+\left(\frac{\mu B}{Kh}\right)\sum_{j=1}^{M}\varepsilon(t-t_{f,j})q_{f,j}\delta(x-x_{f,j})\delta(y-y_{f,j}) \\ &+\left(\frac{\mu B}{Kh}\right)\sum_{i=1}^{N}\varepsilon(t-t_{p,i})q_{p,i}(t)\delta(x-x_{p,i})\delta(y-y_{p,i})s\end{aligned} \tag{2}$$

where P is pressure in the reservoir, $q_{p,i}(t)$ is the transient flow rate of the well i in the first group at time t, $q_{f,j}$ is the constant flow rate of the well j in the second group, ϕ is porosity, μ is viscosity, h is payzone thickness, K is permeability; C_t is the total reservoir compressibility, B is formation volume factor, and

$$\varepsilon(t-t_{p,i})=\begin{cases}1, & \text{if } t\geq t_{p,i}\\ 0, & \text{if } t<t_{p,i}\end{cases},\quad \varepsilon(t-t_{f,j})=\begin{cases}1, & \text{if } t\geq t_{f,j}\\ 0, & \text{if } t<t_{f,j}\end{cases}$$

Note that, the reservoir has constant initial pressure everywhere:

$$P(t,x,y)\Big|_{t=0}=P_{\text{ini}} \tag{3}$$

All the reservoir boundaries are impermeable:

$$\frac{\partial P}{\partial x}\Big|_{x=0,a}=\frac{\partial P}{\partial y}\Big|_{y=0,b}=\frac{\partial P}{\partial z}\Big|_{z=0,h}=0 \tag{4}$$

The wells in the first group are produced at constant but different flowing bottomhole pressures:

$$P(t,x_{p,i},y_{p,i})=P_{wp,i},\quad (i=1,2,\cdots,N) \tag{5}$$

The wells in the second group are produced at constant but different flow rates:

$$q(t,x_{f,j},y_{f,j})=q_{f,j},\quad (j=1,2,\cdots,M) \tag{6}$$

2.3 Dimensionless transformation

To simplify the governing equation, we define the following dimensionless groups (Lu et al., 2018):

$$X_D=\frac{X}{h},\quad Y_D=\frac{Y}{h},\quad h_D=\frac{h}{h}=1 \tag{7}$$

$$t_D=\frac{Kt}{\phi\mu C_t h^2} \tag{8}$$

$$P_D=\frac{2\pi Kh(P_{\text{ini}}-P)}{\mu B q_{\text{ref}}} \tag{9}$$

$$q_{pD,i}(t_D)=\frac{2\pi q_{p,i}(t)}{q_{\text{ref}}},\quad q_{fD,j}=\frac{2\pi q_{f,j}}{q_{\text{ref}}} \tag{10}$$

where P_{ini} is initial reservoir pressure, q_{ref} is the reference flow rate.

Consequently, the governing equation can be denoted as follows:

$$\begin{aligned}&\frac{\partial P_D}{\partial t_D}-\left(\frac{\partial^2 P_D}{\partial X_D^2}+\frac{\partial^2 P_D}{\partial Y_D^2}\right)\\&=\sum_{i=1}^{N}\varepsilon(t_D-t_{pD,i})q_{pD,i}(t_D)\delta(X_D-X_{pD,i})\delta(Y_D-Y_{pD,i})\\&\quad+\sum_{j=1}^{M}\varepsilon(t_D-t_{fD,j})q_{fD,j}\delta(X_D-X_{fD,j})\delta(Y_D-Y_{fD,j})\end{aligned} \tag{11}$$

And then, the dimensionless boundary conditions, initial condition, dimensionless wellbore pressure and flow rate can be expressed as follows:

$$\frac{\partial P_D}{\partial X_D}\Big|_{x=0,a_D}=\frac{\partial P_D}{\partial Y_D}\Big|_{y=0,b_D}=\frac{\partial P_D}{\partial Z_D}\Big|_{z=0,h_D}=0 \tag{12}$$

$$P_D(x_D,y_D)\Big|_{t_D=0}=0 \tag{13}$$

$$P_D(t_D,X_{pD,i},Y_{pD,i})=P_{wpD,i},\quad (i=1,2,\cdots,N) \tag{14}$$

$$q_D(t_D,X_{fD,j},Y_{fD,j})=q_{fD,j},\quad (j=1,2,\cdots,M) \tag{15}$$

2.4 Laplace transform

In order to solve equations in the real space, it's quite convenient to process the equation in the Laplace transform space. Considering the initial condition Eq. (13), taking the Laplace transform with respect to t_D at the both sides of Eq. (11), we obtain (Tuma, 1971; Lu et al., 2018)

$$\begin{aligned}&s\hat{P}_D-\left(\frac{\partial^2\hat{P}_D}{\partial x_D^2}+\frac{\partial^2\hat{P}_D}{\partial y_D^2}\right)\\&=\sum_{i=1}^{N}\exp(-st_{pD,i})\,\hat{q}_{pD,i}(s)\delta(x_D-x_{pD,i})\delta(y_D-y_{pD,i})\\&\quad+\sum_{j=1}^{M}\exp(-st_{fD,j})\left(\frac{q_{fD,j}}{s}\right)\delta(x_D-x_{fD,j})\delta(y_D-y_{fD,j})\end{aligned} \tag{16}$$

Through the superposition principle (Lee et al., 2003; Lu et al., 2012), we can easily obtain the solution of Eq. (16) as below:

$$\begin{aligned}&\hat{P}_D(s,x_D,y_D)\\&=\sum_{i=1}^{N}\exp(-st_{pD,i})\hat{q}_{pD,i}(s)G(s,x_D,y_D;x_{pD,i},y_{pD,i})\\&\quad+\sum_{j=1}^{M}\exp(-st_{fD,j})\left(\frac{q_{fD,j}}{s}\right)G(s,x_D,y_D;x_{fD,j},y_{fD,j})\end{aligned} \tag{17}$$

where (Myint-U and Debnath, 2007; Cole et al., 2010)

$$\begin{aligned}&G(s,x_D,y_D;x_{pD,i},y_{pD,i})=\\&\frac{\sum_{u=0}^{\infty}\sum_{v=0}^{\infty}\cos\left(\frac{u\pi x_D}{a_D}\right)\cos\left(\frac{v\pi y_D}{b_D}\right)\cos\left(\frac{u\pi x_{pD,i}}{a_D}\right)\cos\left(\frac{v\pi y_{pD,i}}{b_D}\right)}{(a_D b_D d_u d_v)(s+\lambda_{uv})}\end{aligned} \tag{18}$$

$$\begin{aligned}&G(s,x_D,y_D;x_{fD,j},y_{fD,j})=\\&\frac{\sum_{u=0}^{\infty}\sum_{v=0}^{\infty}\cos\left(\frac{u\pi x_D}{a_D}\right)\cos\left(\frac{v\pi y_D}{b_D}\right)\cos\left(\frac{u\pi x_{fD,j}}{a_D}\right)\cos\left(\frac{v\pi y_{fD,j}}{b_D}\right)}{(a_D b_D d_u d_v)(s+\lambda_{uv})}\end{aligned} \tag{19}$$

$$d_u=\begin{cases}1, & \text{if } u=0\\ \frac{1}{2}, & \text{if } u>0\end{cases}\quad d_v=\begin{cases}1, & \text{if } v=0\\ \frac{1}{2}, & \text{if } v>0\end{cases} \tag{20}$$

$$\lambda_{uv}=\left(\frac{u\pi}{a_D}\right)^2+\left(\frac{v\pi}{b_D}\right)^2 \tag{21}$$

Note that the flowing bottomhole pressure of each well in the first group is constant, then in Eq. (17), we let $(X_D,Y_D)=(X_{pD,k},Y_{pD,k}),k=1,2,\ldots,N$, there holds:

$$\begin{aligned}&\frac{P_{wpD,k}}{s}-\sum_{j=1}^{M}\frac{q_{fD,j}}{s}G(s,x_{pD,k},y_{pD,k};x_{fD,j},y_{fD,j})\exp(-st_{fD,j})\\&=\sum_{i=1}^{N}\hat{q}_{pD,i}(s)G(s,x_{pD,k},y_{pD,k};x_{pD,i},y_{pD,i})\exp(-st_{pD,i})\end{aligned} \tag{22}$$

or expressed in the matrix form (Zwillinger, 1996):

$$\vec{\hat{P}}_{wD}=\vec{\hat{G}}\vec{\hat{q}}_D \tag{23}$$

where

$$\vec{P}_{wD}=\begin{bmatrix}\frac{P_{wpD,1}}{s}-\sum_{j=1}^{M}\frac{q_{fD,j}}{s}G(s,x_{pD,1},y_{pD,1};x_{fD,j},y_{fD,j})\exp(-st_{fD,j})\\ \frac{P_{wpD,2}}{s}-\sum_{j=1}^{M}\frac{q_{fD,j}}{s}G(s,x_{pD,2},y_{pD,2};x_{fD,j},y_{fD,j})\exp(-st_{fD,j})\\ \vdots\\ \frac{P_{wpD,N}}{s}-\sum_{j=1}^{M}\frac{q_{fD,j}}{s}G(s,x_{pD,N},y_{pD,N};x_{fD,j},y_{fD,j})\exp(-st_{fD,j})\end{bmatrix} \tag{24}$$

$$\vec{\hat{q}}_D(s)=\begin{bmatrix}\exp(-st_{pD,1})\hat{q}_{pD,1}(s)\\ \exp(-st_{pD,2})\hat{q}_{pD,2}(s)\\ \vdots\\ \exp(-st_{pD,N})\hat{q}_{pD,N}(s)\end{bmatrix} \tag{25}$$

and

$$\vec{\hat{G}}=\begin{pmatrix}\hat{G}_{11} & \cdots & \hat{G}_{1N}\\ \vdots & \ddots & \vdots\\ \hat{G}_{N1} & \cdots & \hat{G}_{NN}\end{pmatrix} \tag{26}$$

where

$$\begin{cases}\hat{G}_{11}=G_{11}(s,x_{pD,1},y_{pD,1};x_{pD,1},y_{pD,1})\\ \hat{G}_{1N}=G_{1N}(s,x_{pD,1},y_{pD,1};x_{pD,N},y_{pD,N})\\ \hat{G}_{N1}=G_{N1}(s,x_{pD,N},y_{pD,N};x_{pD,1},y_{pD,1})\\ \hat{G}_{NN}=G_{NN}(s,x_{pD,N},y_{pD,N};x_{pD,N},y_{pD,N})\end{cases}$$

$$G(s,x_{pD,m},y_{pD,m};x_{pD,n},y_{pD,n})=\frac{\sum_{u=0}^{\infty}\sum_{v=0}^{\infty}\cos\left(\frac{u\pi x_{pD,m}}{a_D}\right)\cos\left(\frac{v\pi y_{pD,m}}{b_D}\right)\cos\left(\frac{u\pi x_{pD,n}}{a_D}\right)\cos\left(\frac{v\pi y_{pD,n}}{b_D}\right)}{(a_Db_Dd_ud_v)(s+\lambda_{uv})} \tag{27}$$

and $m,n=1,2,3,\ldots,N$.

In Eq. (24), we have:

$$G(s,x_{pD,i},y_{pD,i};x_{pD,j},y_{pD,j})=\frac{\sum_{u=0}^{\infty}\sum_{v=0}^{\infty}\cos\left(\frac{u\pi x_{pD,i}}{a_D}\right)\cos\left(\frac{v\pi y_{pD,i}}{b_D}\right)\cos\left(\frac{u\pi x_{pD,j}}{a_D}\right)\cos\left(\frac{v\pi y_{pD,j}}{b_D}\right)}{(a_Db_Dd_ud_v)(s+\lambda_{uv})} \tag{28}$$

where $i=1,2,3,\ldots,N, j=1,2,3,\ldots,M$.

Note that:

$$\begin{aligned}&G(s,x_{pD,m},y_{pD,m};x_{pD,n},y_{pD,n})\\ &=\frac{\sum_{u=0}^{\infty}\cos\left(\frac{u\pi x_{pD,m}}{a_D}\right)\cos\left(\frac{u\pi x_{pD,n}}{a_D}\right)}{(2a_Dd_u\omega_u)\sinh(\omega_ub_D)}\\ &\times\{\cosh[\omega_u(b_D-|y_{pD,m}-y_{pD,n}|)]\\ &+\cosh[\omega_u(b_D-(y_{pD,m}+y_{pD,n}))]\}\end{aligned} \tag{29}$$

and

$$\omega_u=\left[s+\left(\frac{u\pi}{a_D}\right)^2\right]^{1/2} \tag{30}$$

If $m=n$, then at the wellbore of well m, there holds:

$$\begin{aligned}G(s,x_{pD,m},y_{pD,m};x_{pD,m},y_{pD,m})&=\sum_{u=0}^{\infty}\left[\cos\left(\frac{u\pi x_{pD,m}}{a_D}\right)\right]^2\\ &\times\frac{\{\cosh[\omega_u(b_D-r_{wpD,m})]+\cosh[\omega_u(b_D-2y_{pD,m})]\}}{(2a_Dd_u\omega_u)\sinh(\omega_ub_D)}\end{aligned} \tag{31}$$

and $m=1,2,3,\ldots,N, r_{wpD,m}$ is the dimensionless wellbore radius of well m which is produced at constant flowing bottomhole pressure $P_{wpD,m}$. We have:

$$\begin{aligned}G(s,x_{pD,i},y_{pD,i};x_{pD,j},y_{pD,j})&=\frac{\sum_{u=0}^{\infty}\cos\left(\frac{u\pi x_{pD,i}}{a_D}\right)\cos\left(\frac{u\pi x_{pD,j}}{a_D}\right)}{(2a_Dd_u\omega_u)\sinh(\omega_ub_D)}\\ &\times\{\cosh[\omega_u(b_D-|y_{pD,i}-y_{pD,j}|)]\\ &+\cosh[\omega_u(b_D-(y_{pD,i}+y_{pD,j})]\}\end{aligned} \tag{32}$$

where $i=1,2,3,\ldots,N, j=1,2,3,\ldots,M$.

2.5 Semi-analytical solution

According to Eqs. (24), (25) and (26), the dimensionless flow rates in the Laplace transform space can be expressed below:

$$\vec{\hat{q}}_D=\left(\vec{\hat{G}}\right)^{-1}\times\vec{\hat{P}}_{wD} \tag{33}$$

$$\vec{\hat{q}}_D=\left(\vec{\hat{G}}\right)^{-1}\times\begin{bmatrix}\frac{P_{wpD,1}}{s}-\sum_{j=1}^{M}\frac{q_{fD,j}}{s}G(s,x_{pD,1},y_{pD,1};x_{fD,j},y_{fD,j})\exp(-st_{fD,j})\\ \frac{P_{wpD,2}}{s}-\sum_{j=1}^{M}\frac{q_{fD,j}}{s}G(s,x_{pD,2},y_{pD,2};x_{fD,j},y_{fD,j})\exp(-st_{fD,j})\\ \vdots\\ \frac{P_{wpD,N}}{s}-\sum_{j=1}^{M}\frac{q_{fD,j}}{s}G(s,x_{pD,N},y_{pD,N};x_{fD,j},y_{fD,j})\exp(-st_{fD,j})\end{bmatrix} \tag{34}$$

The dimensionless cumulative production of well k in the second group which is produced at constant flowing bottomhole pressure $P_{wp,k}$ is given by:

$$Q_{pD,k}(t_D)=\int_0^{t_D}q_{pD,k}(\tau)d\tau \tag{35}$$

Taking the Laplace transform with respect to t_D at the both sides of Eq. (35), we obtain:

$$\hat{Q}_{pD,k}(s)=\frac{\hat{q}_{pD,k}(s)}{s} \tag{36}$$

or

$$\vec{\hat{Q}}_D(s)=\begin{bmatrix}\exp(-st_{pD,1})\hat{q}_{pD,1}(s)/s\\ \exp(-st_{pD,2})\hat{q}_{pD,2}(s)/s\\ \vdots\\ \exp(-st_{pD,N})\hat{q}_{pD,N}(s)/s\end{bmatrix}=\left(\vec{\hat{G}}\right)^{-1}\times$$

$$\begin{bmatrix} \frac{P_{wpD,1}}{s^2} - \sum_{j=1}^{M} \frac{q_{fD,j}}{s^2} G(s,x_{pD,1},y_{pD,1};x_{fD,j},y_{fD,j}) \exp(-st_{fD,j}) \\ \frac{P_{wpD,2}}{s^2} - \sum_{j=1}^{M} \frac{q_{fD,j}}{s^2} G(s,x_{pD,2},y_{pD,2};x_{fD,j},y_{fD,j}) \exp(-st_{fD,j}) \\ \vdots \\ \frac{P_{wpD,N}}{s^2} - \sum_{j=1}^{M} \frac{q_{fD,j}}{s^2} G(s,x_{pD,N},y_{pD,N};x_{fD,j},y_{fD,j}) \exp(-st_{fD,j}) \end{bmatrix} \tag{37}$$

Now an analytical model for predicting transient flow rates of multiple wells producing at constant bottomhole pressures during boundary-dominated flow period in a closed rectangular reservoir has been established. However, the solutions to the model are in the Laplace transform space. By using the numerical inversion method developed by Stehfest (1970), we can convert these solutions from the Laplace transform space into the real time space.

3. Simplified analytical model

Assume no well is produced at constant flow rate, all wells are produced at constant but different flowing bottomhole pressures, and all wells begin to produce at the same time. Well i is located at (x_i, y_i), $i = 1, 2, \ldots, N$. Then Eq. (2) can be simplified as below:

$$\frac{\partial^2 P}{\partial x^2} + \frac{\partial^2 P}{\partial y^2} = \left(\frac{\phi \mu C_t}{K}\right) \frac{\partial P}{\partial t} + \left(\frac{\mu B}{Kh}\right) \sum_{i=1}^{N} q_i(t) \delta(x - x_i) \delta(y - y_i) \tag{38}$$

The reservoir initial condition is Eqs. (3); the reservoir outer boundary condition is Eq. (4).

Well i is produced at constant flowing bottomhole pressure $P_{w,i}$:

$$P(t, x_i, y_i) = P_{w,i}, \quad (i = 1, 2, \cdots, N) \tag{39}$$

In the dimensionless space, we have:

$$\frac{\partial P_D}{\partial t_D} - \left(\frac{\partial^2 P_D}{\partial x_D^2} + \frac{\partial^2 P_D}{\partial y_D^2}\right) = \sum_{i=1}^{N} q_{D,i}(t_D) \delta(x_D - x_{D,i}) \delta(y_D - y_{D,i}) \tag{40}$$

Taking the Laplace transform with respect to t_D at the both sides of Eq. (40), we obtain:

$$s\hat{P}_D - \left(\frac{\partial^2 \hat{P}_D}{\partial x_D^2} + \frac{\partial^2 \hat{P}_D}{\partial y_D^2}\right) = \sum_{i=1}^{N} \hat{q}_{D,i}(s) \delta(x_D - x_{D,i}) \delta(y_D - y_{D,i}) \tag{41}$$

The solution of Eq. (41) is given by:

$$\hat{P}_D(s, x_D, y_D) = \sum_{i=1}^{N} \hat{q}_{D,i}(s) G(s, x_D, y_D; x_{D,i}, y_{D,i}) \tag{42}$$

Note that the flowing bottomhole pressure of each well is constant, then in Eq. (42) we let $(x_D, y_D) = (x_{D,k}, y_{D,k})$, $k = 1, 2, 3, \ldots, N$, there holds:

$$\frac{P_{wpD,k}}{s} = \sum_{i=1}^{N} \hat{q}_{D,i}(s) G(s, x_{D,k}, y_{D,k}; x_{D,i}, y_{D,i}) \tag{43}$$

We can use the matrix form Eq. (43) to express the above equation, and

$$\vec{\hat{p}}_{wD} = \begin{bmatrix} \frac{P_{wpD,1}}{s} \\ \frac{P_{wpD,2}}{s} \\ \vdots \\ \frac{P_{wpD,N}}{s} \end{bmatrix}, \qquad \vec{\hat{q}}_D(s) = \begin{bmatrix} \hat{q}_{D,1}(s) \\ \hat{q}_{D,2}(s) \\ \vdots \\ \hat{q}_{D,N}(s) \end{bmatrix} \tag{44}$$

$$\vec{\tilde{G}} = \begin{pmatrix} \tilde{G}_{11} & \cdots & \tilde{G}_{1N} \\ \vdots & \ddots & \vdots \\ \tilde{G}_{M1} & \ldots & \tilde{G}_{MN} \end{pmatrix} \tag{45}$$

where

$$\begin{cases} \tilde{G}_{11} = G_{11}(s, x_{D,1}, y_{D,1}; x_{D,1}, y_{D,1}) \\ \tilde{G}_{1N} = G_{1N}(s, x_{D,1}, y_{D,1}; x_{D,N}, y_{D,N}) \\ \tilde{G}_{M1} = G_{M1}(s, x_{D,N}, y_{D,N}; x_{D,1}, y_{D,1}) \\ \tilde{G}_{MN} = G_{MN}(s, x_{D,N}, y_{D,N}; x_{D,N}, y_{D,N}) \end{cases}$$

and we have:

$$G(s, x_{D,i}, y_{D,i}; x_{D,j}, y_{D,j}) = \frac{\sum_{u=0}^{\infty} \cos\left(\frac{u\pi x_{D,i}}{a_D}\right) \cos\left(\frac{u\pi x_{D,j}}{a_D}\right)}{(2a_D d_u \omega_u) \sinh(\omega_u b_D)} \times \{\cosh[\omega_u(b_D - |y_{D,i} - y_{D,j}|] + \cosh[\omega_u(b_D - (y_{D,i} + y_{D,j}))\} \tag{46}$$

$$G(s, x_{D,i}, y_{D,i}; x_{D,i}, y_{D,i}) = \frac{\sum_{u=0}^{\infty} \left[\cos\left(\frac{u\pi x_{D,i}}{a_D}\right)\right]^2}{(2a_D d_u \omega_u) \sinh(\omega_u b_D)} \times \{\cosh[\omega_u(b_D - r_{wD,i})] + \cosh[\omega_u(b_D - 2y_{D,i})]\} \tag{47}$$

The dimensionless flow rates in the Laplace transform space can be expressed below:

$$\begin{bmatrix} \hat{q}_{D,1}(s) \\ \hat{q}_{D,2}(s) \\ \vdots \\ \hat{q}_{D,N}(s) \end{bmatrix} = \left(\vec{\tilde{G}}\right)^{-1} \times \begin{bmatrix} \frac{P_{wpD,1}}{s} \\ \frac{P_{wpD,2}}{s} \\ \vdots \\ \frac{P_{wpD,N}}{s} \end{bmatrix} \tag{48}$$

The dimensionless cumulative production in the Laplace transform space is

$$\vec{\hat{Q}}_D(s) = \begin{bmatrix} \frac{\hat{q}_{D,1}(s)}{s} \\ \frac{\hat{q}_{D,2}(s)}{s} \\ \vdots \\ \frac{\hat{q}_{D,N}(s)}{s} \end{bmatrix} = \left(\vec{\tilde{G}}\right)^{-1} \times \begin{bmatrix} \frac{P_{wD,1}}{s^2} \\ \frac{P_{wD,2}}{s^2} \\ \vdots \\ \frac{P_{wD,N}}{s^2} \end{bmatrix} \tag{49}$$

4. Validation

Computer Modeling Group Ltd., abbreviated as CMG, develops market-leading reservoir simulation software, which is known as the industry standard for advanced recovery processes. In this paper, the CMG Black oil simulator IMEX is used to build and run the simulation. And we will use the proposed analytical model to investigate the production performance of a three-wells system in a closed square-shaped reservoir, as shown in Fig. 1. The input reservoir data, formation properties and fluid properties data are shown in Table 1. We assume the lower left point of the square is the origin point of the Cartesian coordinate system, then Well A is at (750 m, 375 m), Well B at (425.24 m, 937.5 m), Well C at (1074.76 m, 937.5 m), as shown in Fig. 1.

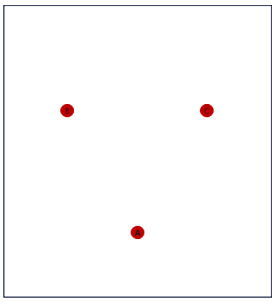

Fig. 1. Three-wells system.

And we assume Well A, Well B and Well C in Figure 1 producing under the same constant bottomhole pressures of 10MPa, thus the production pressure difference of each well is identical and keeps a constant during production, $P_{ini} - P_{wf} = \Delta P_w = 5$ MPa.

Note that the positions of Well A, Well B and Well C form an equilateral triangle, the three wells are equidistant from the center of the square reservoir and producing under the equal production pressure difference, so at a given time, their transient flow rates are identical. By using the IMEX simulator, we can obtain the transient flow rate of the three production wells. Through the proposed model, we can calculate the dimensionless flow rate of Well A in the same case as the CMG simulation. Recall Eqs. (8) and (10), if we use practical units, (h in m; K in mPa·s; K in μm^2; C_t in MPa^{-1}; t in day; $q(t)$ and q_{ref} in Sm^3/day) then the dimensionless production time and the dimensionless flow rate can be converted to the production time and the flow rate as below:

$$t = \frac{\phi \mu C_t h^2 t_D}{86.4K} \tag{50}$$

$$q(t) = \frac{q_D(t_D) \times q_{\text{ref}}}{2\pi} \tag{51}$$

Then, the calculated flow rate and flow rate obtained by the CMG simulation can be compared, as shown in Fig. 2.

It can be found from the figure that the transient flow rate predicted by the proposed model is basically consistent with the overall trend of the transient flow rate obtained by the CMG simulation over time, indicating that the results predicted by the proposed model are reliable within a certain range. Since we ignore the high order term in the model development for multi-well system, and the numerical inverse Laplace transform method proposed by Stehfest (1970) is an approximate method, consequently, there exist some differences between the CMG simulation and the proposed model results. But the differences are not significant.

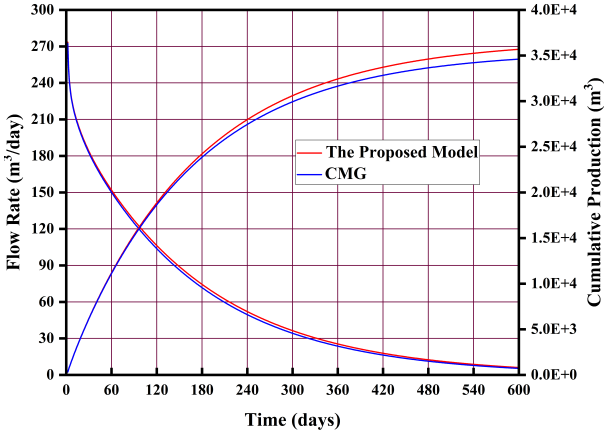

Fig. 2. Comparison of the transient flow rate obtained by the CMG simulation and the proposed model of Well A.

5. Application and analysis

In this part, we will use the proposed model to study the effects of number of wells, well arrangement style, reservoir size, bottomhole pressure difference and well production starting time on the production performance of a multi-well system.

5.1 The effect of number of wells

Example 1: We study the effect of number of wells on production performance. The reservoir data, formation properties and fluid properties data are given in Table 1, and the production pressure difference of each well is identical and keeps a constant during production, $\Delta P_w = 5$ MPa. Calculate the transient flow rates of Well A in the following cases.

Case 1: Only Well A is located at the center of the square-shaped reservoir, as shown in Fig. 3.

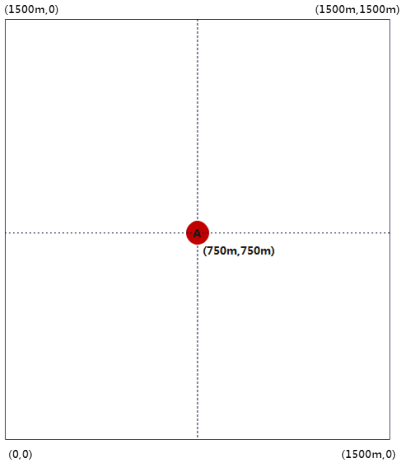

Fig. 3. One-well system in a square reservoir.

Table 1. Reservoir and fluid properties data.

Reservoir domain, Ω	1500 m × 1500 m
Initial reservoir pressure, P_{ini}	15 MPa
Formation volume factor, B	1.15 Rm^3/Sm^3
Reservoir thickness, h	25 m
Reservoir porosity, ϕ	0.15
Reservoir permeability, K	0.1 μm^2
Total reservoir compressibility, C_t	3.0 × 10^{-3} MPa^{-1}
Oil viscosity, μ	5 mPa·s
Production time prior to shut-in, t_p	720 hours
Wellbore radius, r_w	0.1 m

Case 2: Two-wells system, Well A is at (750 m, 750 m), Well B at (750 m, 1125 m), as shown in Fig. 4.

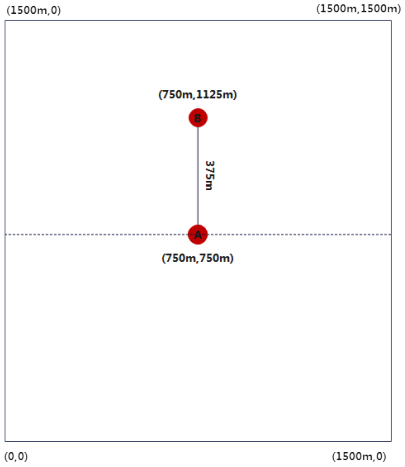

Fig. 4. Two-wells system in a square reservoir.

Case 3: Four-wells system, Well A at (750 m, 750 m), Well B at (750 m, 375 m), Well C at (425.24 m, 937.5 m), Well D at (1074.76 m, 937.5 m), as shown in Fig. 5.

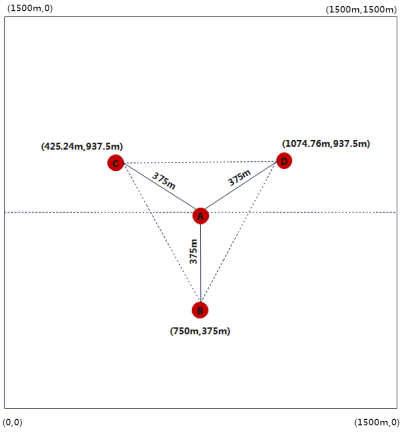

Fig. 5. Four-wells system in a square reservoir.

Case 4: Five-wells system, Well A at (750 m, 750 m), Well B at (484.83 m, 484.83 m), Well C at (484.83 m, 1015.17 m), Well D at (1015.17 m, 1015.17 m), Well E at (1015.17 m, 484.83 m), as shown in Fig. 6.

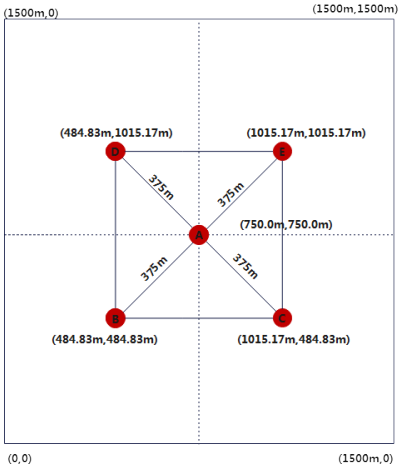

Fig. 6. Five-wells system in a square reservoir.

The transient flow rates of Well A in the above four cases are shown in Figs. 7 and 8.

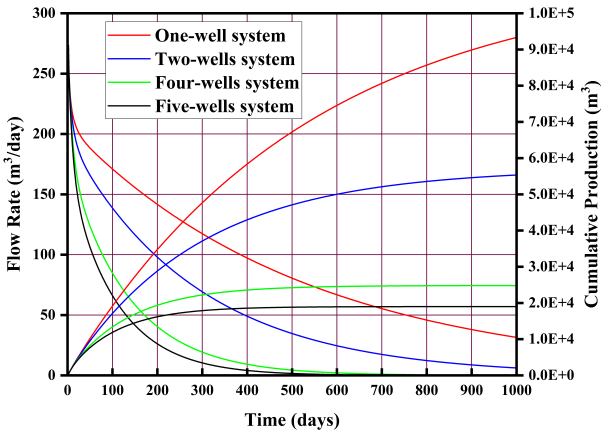

Fig. 7. Cartesian plot of flow rate and cumulative production of Well A in the square reservoir with different numbers of wells.

As can be seen from Figs. 4, 5 and 6, the inter-well distance

between **Well A** and its adjacent wells is identical and equal to 375 m. As can be seen from Figs. 7 and 8, at a given time, with the increase of the number of wells, the flow rate of **Well A** decreases. Decline rate is defined as the slope of straight line segment on the semi-log plot of q vs. t. It can be seen from Fig. 8, the slope of the straight line segment in **Case 4** (Five-wells system) is the largest, the slope of the straight line segment in **Case 1** (One-well system) is the smallest. At any time, with the increase of the number of wells, the drainage area of **Well A** decreases, the interference degree of adjacent wells to **Well A** increases, and the energy consumption degree of the reservoir increases, which leads to the decrease of transient flow rate and the increase of decline rate of **Well A**.

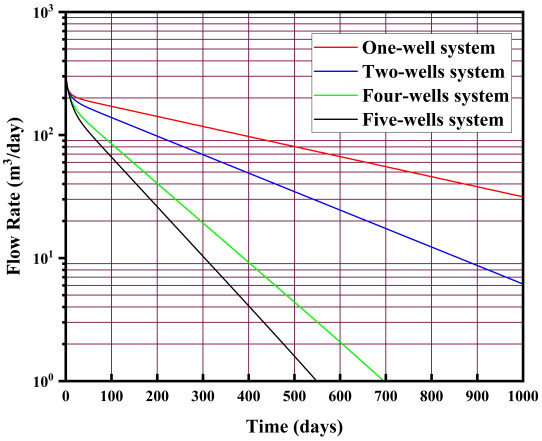

Fig. 8. Semi-log plot of flow rate of Well A in the square reservoir with different numbers of wells.

5.2 The effect of well arrangement style

Example 2: We study the effect of well arrangement style on production performance. The reservoir data, formation properties and fluid properties data are given in Table 1, and the production pressure difference of each well is identical and keeps a constant during production, ΔP_w = 5 MPa. Calculate the transient flow rates of **Well A** in the following cases.

Case 1: Well A at (750 m, 375 m), Well B at (425.24 m, 937.5 m), Well C at (1074.76 m, 937.5 m), the three wells form an equilateral triangle, as shown in Fig. 9.

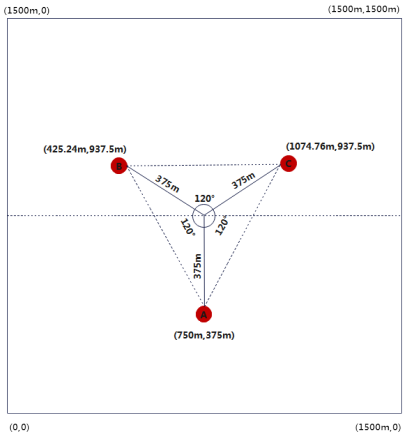

Fig. 9. Three-wells system arranged as an equilateral triangle.

Case 2: Well A at (750 m, 750 m), Well B at (375 m, 750 m), Well C at (1125 m, 750 m), the three wells are at positions half height of the square-shaped reservoir, they are in a straight line parallel to the bottom edge of the square, as shown in Fig. 10.

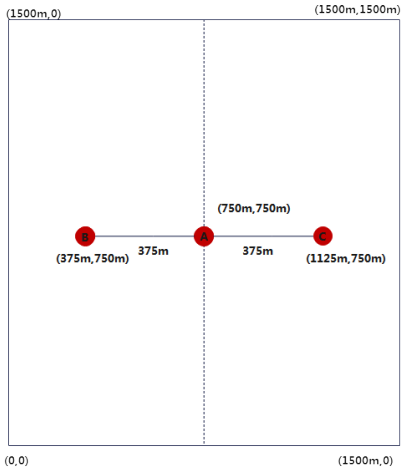

Fig. 10. Three-wells system arranged at half height of the square.

Case 3: Well A at (750 m, 750 m), Well B at (484.83 m, 484.83 m), Well C at (1015.17 m, 1015.17 m), the three wells are arranged along the diagonal of the square-shaped reservoir, as shown in Fig. 11.

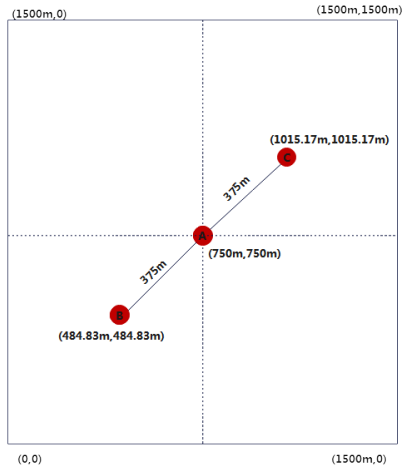

Fig. 11. Three-wells system arranged along the diagonal of the square.

The transient flow rates of **Well A** in the above three cases are shown in Figs. 12 and 13.

As can be seen from Figs. 12 and 13, in the early days, the production performance of **Well A** is almost the same in the above three cases. When production time is larger than 300 days, the slope of the straight line segment in **Case 1** (equilateral triangle well arrangement) is the largest. The distance between **Well A** and the bottom edge of the square is 375 m in **Case 1** . **Well A** is at the center of the square reservoir in **Case 2** (half-height well arrangement) and in **Case 3** (diagonal well arrangement), the distance between **Well A** and each closed boundary is the same and equal to

750 m, the effects of the four boundaries can cancel each other out in **Case 2** and **Case 3** . Compared with well interference effects, the boundary effect from the bottom closed boundary has greater influence on flow rate although the inter-well distance in **Case 1** is larger than that in **Case 2** and **Case 3** , which leads to the smallest transient flow rate and the largest the decline rate of **Well A** in **Case 1** at a large time (more than 300 days).

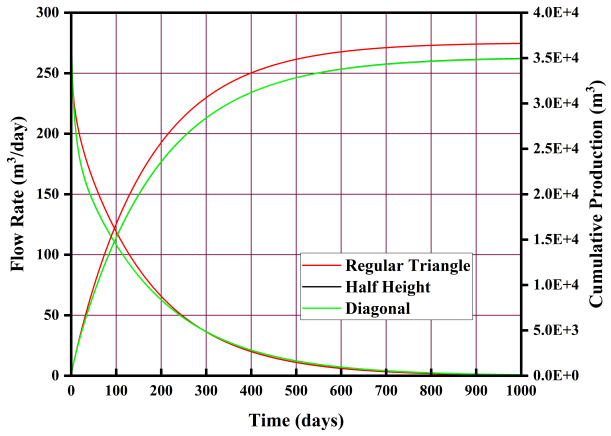

Fig. 12. Cartesian plot of flow rate and cumulative production of Well A in the three-wells system with different well patterns.

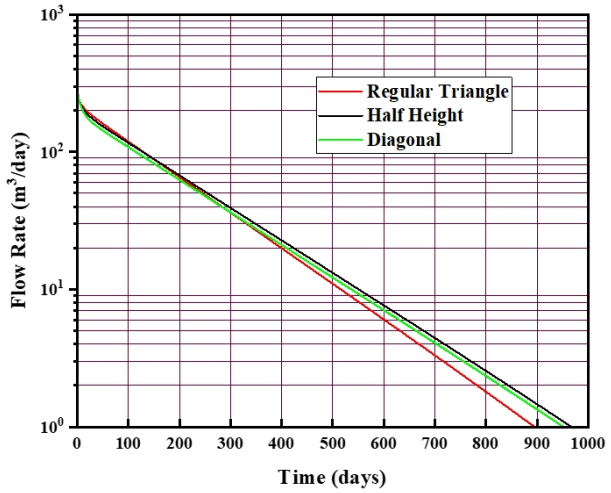

Fig. 13. Semi-log plot of flow rate of Well A in the three-wells system with different well patterns.

Example 3: We study the effect of inter-well distance on production performance. Suppose Well A, Well B and Well C form an equilateral triangle in a square-shaped reservoir, the positions of the three wells are symmetric with respect to the reservoir boundaries (see Fig. 1). The production pressure difference of each well is identical and keeps a constant during production, ΔP_w = 5 MPa. The reservoir data, formation properties and fluid properties data are given in Table 1. Calculate the transient flow rates of each well when the inter-well distance is 100, 200, 300 and 400 m, respectively.

Obviously, at a given time the transient flow rates of the three wells are equal to each other due to symmetric well locations in the square reservoir. The transient flow rates of **Well A** in the above four cases are shown in Figs. 14 and 15.

As can be seen from Figs. 14 and 15, if production time is less than 200 days, the larger the inter-well distance, the larger the transient flow rate, and the smaller the decline rate. With the increase of inter-well distance, the degree of interference between wells is reduced, consequently the energy consumption degree of the reservoir decreases, and production decline rate is also reduced. At a large time (more than 200 days), pressure transient has reached boundaries, with the increase of inter-well distance, the distance between **Well A** and the bottom edge of the square decreases (see Fig. 1), the boundary effects become more pronounced, which leads to the decrease of transient flow rate and the increase of decline rate of **Well A** .

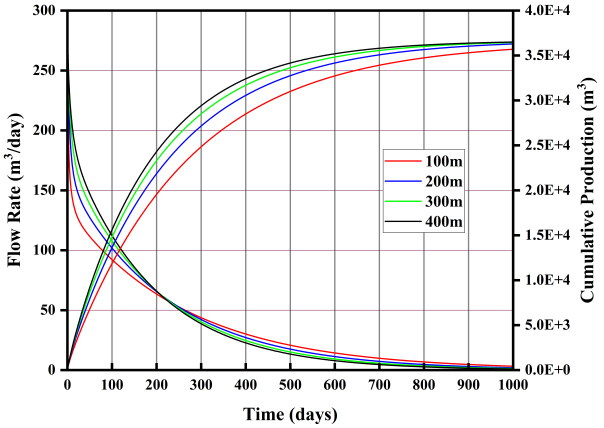

Fig. 14. Cartesian plot of flow rate and cumulative production of Well A in the three-wells system with different inter-well distances.

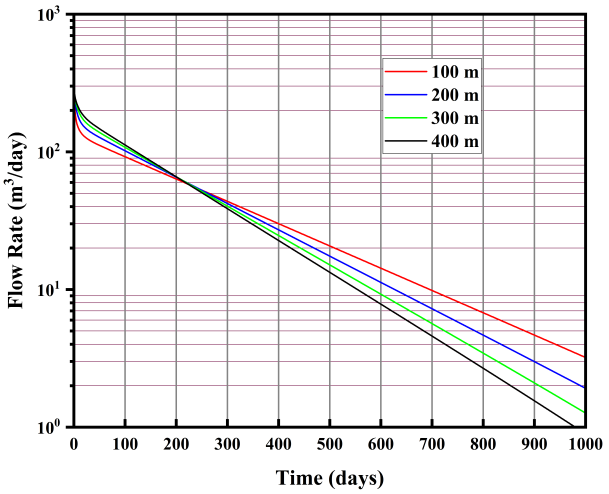

Fig. 15. Semi-log plot of flow rate of Well A in the three-wells system with different inter-well distances.

5.3 The effect of reservoir size

Example 4: We study the effect of reservoir size on production performance. Suppose Well A, Well B and Well

C form an equilateral triangle in a square-shaped reservoir, the positions of the three wells are symmetric with respect to the reservoir boundaries (see Fig. 1). The production pressure difference of each well is identical and keeps a constant during production, ΔP_w = 5 MPa. The reservoir data, formation properties and fluid properties data are given in Table 1. Calculate the transient flow rates of each well when the reservoir size is 1500 m × 1500 m, 1750 m × 1750 m, 2000 m × 2000 m and 2500 m × 2500 m, respectively.

Obviously, for a given reservoir size and at a given time, the transient flow rates of the three wells are equal to each other due to symmetric well locations in the square reservoir. The transient flow rates of **Well A** in the above four cases are shown in Figs. 16 and 17.

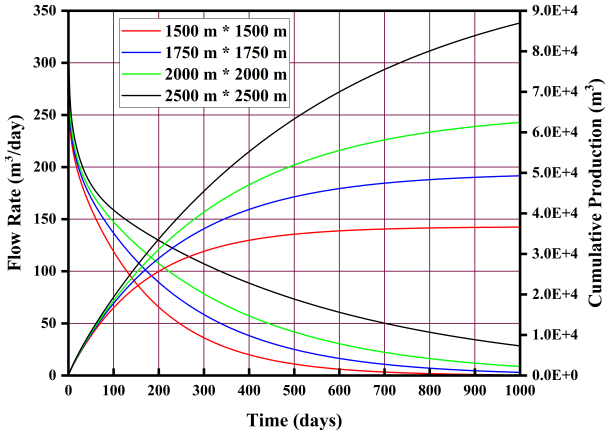

Fig. 16. Cartesian plot of flow rate and cumulative production of Well A in the three-wells system with different reservoir sizes.

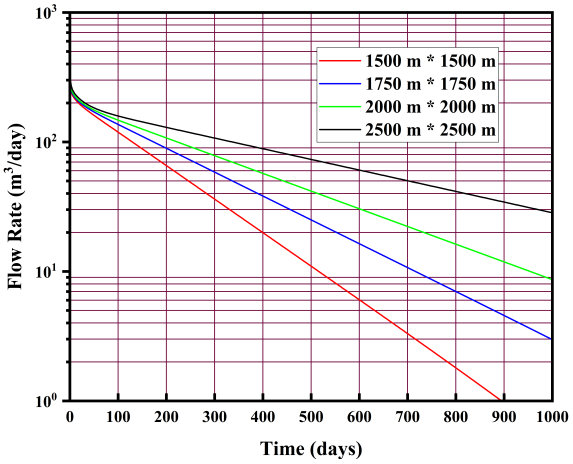

Fig. 17. Semi-log plot of flow rate of Well A in the three-wells system with different reservoir sizes.

As can be seen from Figs. 16 and 17, at a given time, the larger the reservoir size, the larger the transient flow rate, and the smaller the decline rate. With the increase of reservoir size is, the drainage area of **Well A** increases, the interference degree of adjacent wells to Well A decreases, which leads to the increase of transient flow rate and the decrease of decline rate of **Well A** .

5.4 The effect of bottomhole pressure difference

Example 5: We study the effect of bottomhole pressure difference on production performance. Suppose Well A, Well B and Well C form an equilateral triangle in a square-shaped reservoir, the positions of the three wells are symmetric with respect to the reservoir boundaries (see Fig. 1). The reservoir data, formation properties and fluid properties data are given in Table 1. Calculate the transient flow rates of **Well A** in the following cases.

Case 1: The bottomhole pressure difference at Well A is 5 MPa, the bottomhole pressure difference at Well B and Well C is identical and equal to 3 MPa. ΔP_{wA} = 5 MPa; ΔP_{wB} = ΔP_{wC} = 3 MPa.

Case 2: The bottomhole pressure difference at Well A is 5 MPa, the bottomhole pressure difference at Well B and Well C is identical and equal to 4 MPa, ΔP_{wA} = 5 MPa; ΔP_{wB} = ΔP_{wC} = 4 MPa.

Case 3: The bottomhole pressure difference at each well is identical and equal to 5 MPa, ΔP_{wA} = ΔP_{wB} = ΔP_{wC} = 5 MPa.

As can be seen from Figs. 18 and 19, at a given time, with the increase of bottomhole pressure difference (production pressure difference) in adjacent wells (Well B and Well C), the interference degree of adjacent wells to **Well A** increases, which leads to the decrease of transient flow rate and the increase of decline rate of **Well A**.

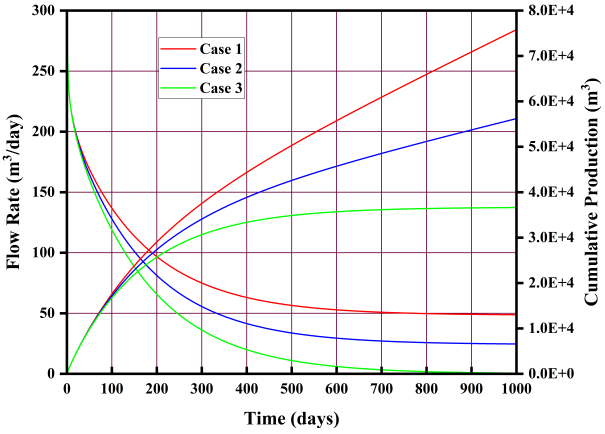

Fig. 18. Cartesian plot of flow rate and cumulative production of Well A in the three-wells system with different bottomhole pressure difference.

5.5 The effect of well production starting time

Assume there are six fully penetrating vertical well in a square-shaped reservoir. The reservoir data, formation properties and fluid properties data are given in Table 1. Three wells in the first group are produced at constant flowing bottom hole pressures, another three wells in the second group are produced at constant flow rates. The data of well locations, wellbore radius, bottomhole pressure difference, flow rates and production starting time are given in Table 2.

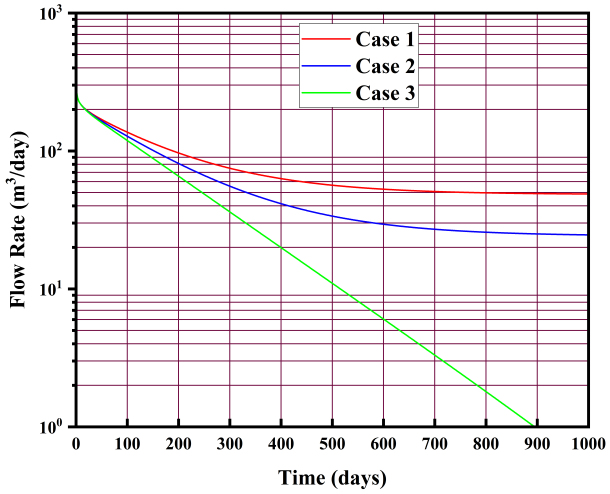

Fig. 19. Semi-log plot of flow rate of Well A in the three-wells system with different bottomhole pressure difference.

Example 6: Calculate the transient flow rates of Well No.1 in the first group, i.e. the well at (500 m, 500 m), compare the calculation results in the following cases:

Case 1: All the data, i.e., the production starting time, bottomhole pressure difference of each well in the first group, flow rate of each well in the second group are the same as those shown in Table 2.

Case 2: The flow rate of each well in the second group is identical and equal to 150 m3/day, other data are same as those shown in Table 2.

Case 3: The production starting time of each well is $t = 0$, other data are same as those shown in Table 2.

Case 4: The production starting time of each well is $t = 0$, and the flow rate of each well in the second group is identical and equal to 150 m^3/day, other data are same as those shown in Table 2.

After 45 days of the production starting time of Well No.1 in the first group, all the six wells have begun to produce in the above four cases. As can be seen from Figs. 20 and 21, when production time is larger than 45 days, if constant flow rate of the three wells in the second group is equal to a small value of 50 m^3/day, there is no significant difference between the transient flow rates in Case 1 and Case 3; if constant flow rate of the three wells in the second group is equal to a large value of 150 m^3/day, there is significant difference between the transient flow rates in Case 2 and Case 4, which leads to the conclusion that only when constant flow rates of the wells in the second group are large, the production starting times of the two group wells have significant influence on production performance on Well No.1.

All the six wells in Case 3 start producing at the same time at $t = 0$, the reservoir energy consumption is relatively large, resulting in a slightly lower flow rate in Case 3 than in Case 1. For the same reason, at a given time, the transient flow rate in Case 4 is smaller than that in Case 2.

But the value of constant flow rates of the three wells in the second group have significant influence on production performance on Well No.1 in the first group. With the increase of flow rate of the wells in the second group from 50 to 150 m^3/day, the energy consumption degree of the reservoir increases, which leads to the decrease of transient flow rate and the increase of decline rate of Well No.1 in Case 2 and Case 4. So, at a given time, the transient flow rate in Case 1 is larger than that in Case 2, and the transient flow rate in Case 3 is larger than that in Case 4. Because all the six wells begin to produce at time $t = 0$ and flow rate of the wells in the second group is 150 m^3/day, the reservoir energy consumption is largest, consequently transient flow rate of Well No.1 at a given time is the smallest in Case 4.

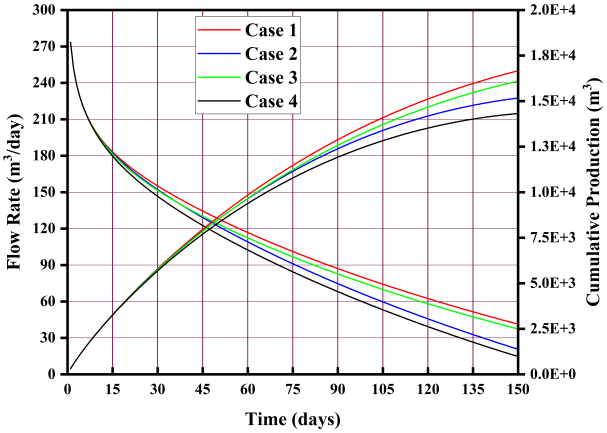

Fig. 20. Cartesian plot of flow rate and cumulative production of Well No.1 in the first group.

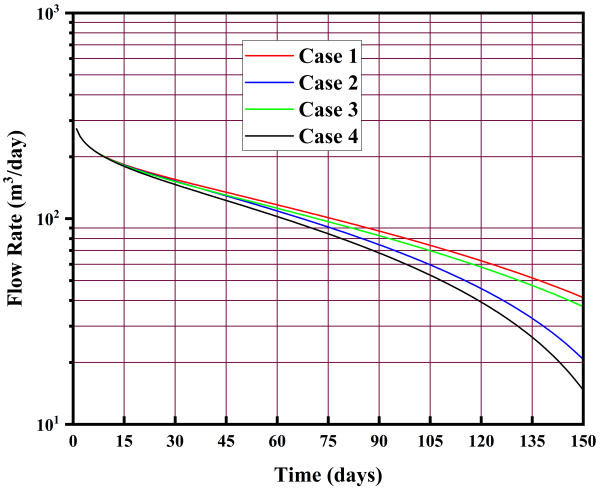

Fig. 21. Semi-log plot of flow rate of Well No.1 in the first group.

6. Conclusions

Compared with the empirical or semi-analytical models in the literature, our proposed model in this paper has a solid theoretical basis, and the proposed analytical model provides a computationally efficient, accurate and convenient method for predicting transient flow rates of multiple wells producing at different constant bottomhole pressures during boundary-dominated flow period in a closed rectangular reservoir. Comparing with the results in the CMG simulation, it is found that the proposed model is accurate enough to predict

Table 2. Well location, wellbore pressure and flow rate data

Wells in the first group		Wells in the second group	
$(x_{p,1}, y_{p,1}) = (500\text{m}, 500\text{m})$	$\Delta P_{wp,1} = 5\text{MPa}$	$(x_{f,1}, y_{f,1}) = (1000\text{m}, 500\text{m})$	$q_{f,1} = 505\text{m}^3/\text{day}$
$(x_{p,2}, y_{p,2}) = (500\text{m}, 750\text{m})$	$\Delta P_{wp,2} = 5\text{MPa}$	$(x_{f,2}, y_{f,2}) = (1000\text{m}, 750\text{m})$	$q_{f,2} = 505\text{m}^3/\text{day}$
$(x_{p,3}, y_{p,3}) = (500\text{m}, 1000\text{m})$	$\Delta P_{wp,3} = 5\text{MPa}$	$(x_{f,3}, y_{f,3}) = (1000\text{m}, 1000\text{m})$	$q_{f,3} = 505\text{m}^3/\text{day}$
$r_w = 0.1$ m		$r_w = 0.1$ m	
$t_{p,1} = 0$		$t_{f,1} = 0$	
$t_{p,2} = 30$ days		$t_{f,2} = 15$ days	
$t_{p,3} = 45$ days		$t_{f,3} = 35$ days	

the production performance of multiple wells under constant bottomhole pressures. Also, the transient flow rates of multiple well systems are affected by the number of wells, the well arrangement style, the reservoir size, the bottomhole pressure difference and the well production starting time.

The following conclusions can be reached:

- In a given reservoir and at a given time, the flow rate of an observation well decreases as the number of total wells increases and bottomhole pressure differences of adjacent wells increase.
- In a given reservoir and at a given time, if the observation well is near a closed boundary, the influence on the flow rate of the boundary is greater than that of the inter-well distance.
- In a given reservoir, if production time is small, the greater distance between the observation well and adjacent wells, the larger the flow rate of the observation well; if production time is large, the greater distance between the observation well and adjacent wells, the smaller the flow rate of the observation well;
- At a given time, the larger the reservoir size, the larger flow rate of the observation well in a multiple-wells system.
- If the multiple-wells system has one group of wells produced at constant bottom hole pressures, another group of wells produced at constant flow rates, notably, only the wells with constant flow rates exhibit high production values, the well production starting time has significant effects on the performance of the observation well.

Nomenclature

a = Length of rectangular reservoir, m
a_D = Dimensionless length of rectangular reservoir
b = Width of rectangular reservoir, m
b_D = Dimensionless width of rectangular reservoir
B = Formation volume factor, Rm^3/Sm^3
C_t = Total reservoir compressibility, MPa^{-1}
h = Formation thickness, m
K = Reservoir permeability, μm^2
P = Pressure, MPa
P_{ini} = Initial reservoir pressure, MPa
P_w = Flowing bottom bore pressure, MPa
P_D = Dimensionless pressure
P_{wD} = Dimensionless flowing bottom bore pressure
$\hat{P}_D$ = Dimensionless pressure in Laplace transform space
Q = Cumulative production, Sm^3
Q_D = Dimensionless cumulative production
$\hat{Q}_D$ = Dimensionless cumulative production in Laplace transform space
q = Flow rate, Sm^3/day
q_D = Dimensionless flow rate
$\hat{q}_D$ = Dimensionless flow rate in Laplace transform space
q_{ref} = Reference flow rate, Sm^3/day
r = Radial distance, m
r_D = Dimensionless radial distance
r_w = Wellbore radius, m
r_{wD} = Dimensionless wellbore radius
t = Time, day
t_D = Dimensionless time
x_i = Coordinate in X direction of well i in rectangular reservoir, m
x_{Di} = Dimensionless coordinate in X direction of well i in rectangular reservoir
y_i = Coordinate in Y direction of well i in rectangular reservoir, m
y_{Di} = Dimensionless coordinate in Y direction of well i in rectangular reservoir

Greek symbols

μ = Fluid viscosity, mPa·s
ϕ = Porosity
λ_{uv} = A function defined by Eq. (21)
ω_u = A function defined by Eq. (30)

Subscripts

D = Dimensionless
f = Constant flow rate production status
ini = Initial
p = Constant bottom hole pressure production status

Acknowledgements

Authors acknowledge the financial supports from the "Local Universities Reformation and Development Personnel Training Project from Central Authorities, Study on nanosystem displacement method of tight reservoir in Daqing Oilfield", and National Natural Science Foundation of China (NSFC) under grant No.52274037, and the Hainan Province Science and Technology Special Fund under grant No. ZDYF2022SHFZ107.

Conflict of interest

The authors declare no competing interest.

References

Agarwal, R. G., Gardner, D. C., Kleinsteiber, S. W., et al. Analyzing well production data using combined type curve and decline curve analysis concepts. Paper SPE 49222 Presented at SPE Annual Technical Conference and Exhibition, New Orleans, Louisiana, 27–30 September, 1998.

Agbi, B., Ng, M. C. A numerical solution to two-parameter representation of production decline curve analysis. Paper SPE 16505 Presented at Petroleum Industry Application of Microcomputers, Lake Conroe, Texas, 23–26 June, 1987.

Anderson, D. M., Thompson, J. M., Behmanesh, H. Diagnosing the health of your well with rate transient analysis. Paper SPE 2902908 Presented at SPE/AAPG/SEG Unconventional Resources Technology Conference, Houston, Texas, USA, 23–25 July, 2018.

Arps, J. J. Analysis of decline curves. Transactions of the American Institute of Mechanical Engineers, 1945, 160(1): 228-247.

Blasingame, T. A., Lee, W. J. Variable-rate reservoir limits testing. Paper SPE 15028 Presented at Permian Basin Oil and Gas Recovery Conference, Midland, Texas, USA, 13-14 March, 1986.

Blasingame, T. A., Johnston, J. L., Lee, W. J. Type curve analysis using the pressure integral method. Paper SPE 18799 Presented at California Regional Meeting, Bakersfield, California, 5-7 April, 1989.

Camacho, R., Raghavan, R. Boundary-dominated flow in solution gas-drive reservoirs. Paper SPE 19009 Presented at Low Permeability Reservoirs Symposium, Denver, Colorado, 6–8 March, 1989.

Cole, K., Beck, J., Haji-Sheikh, A., et al. Heat conduction using Greens functions. New York City, USA, CRC Press Taylor and Francis Group, 2010.

Duong, A. N. An unconventional rate decline approach for tight and fracture-dominated gas wells. Paper SPE 137748 Presented at Canadian Unconventional Resources and International Petroleum Conference, Calgary, Alberta, Canada, 19–21 October, 2010.

Ehlig-Economides, C. A., Ramey, H. J., Transient rate decline analysis for wells produced at constant pressure. Society of Petroleum Engineers Journal, 21(1): 98-104.

Ezabadi, M. G., Ataei, A., Liang, T. K., et al. Production data analysis for reservoir characterization in conventional gas fields: A new workflow and case study. Paper SPE 186270 Presented at SPE/IATMI Asia Pacific Oil and Gas Conference and Exhibition, Jakarta, Indonesia, 17-19 October, 2017.

Fetkovich, M. J. Decline curve analysis using type curves Paper SPE 4629 Presented at Fall Meeting of the Society of Petroleum Engineers of AIME, Las Vegas, Nevada, September 30-October 3, 1973.

Hassanzadeh, H., Pooladi-Darvish, M. Comparison of different numerical Laplace inversion methods for engineering applications. Applied Mathematics and Computation, 2007, 189(2): 1966-1981.

Hu, C., Lu, J., He, X. Productivity formulae of an infinite-conductivity hydraulically fractured well producing at constant wellbore pressure based on numerical solutions of a weakly singular integral equation of the first kind. Mathematical Problems in Engineering, 2012, 2012(1): 428596.

Hurst, W. Unsteady flow of fluids in oil reservoirs. Journal of Applied Physics, 1934, 5(1): 20-30.

Jha, H. S., Khanal, A., Lee, W. J. Effect of errors in initial pressure measurement on rate-transient analysis in unconventional reservoirs. Paper SPE 208321 Presented at Asia Pacific Unconventional Resources Technology Conference, 16-18 November, 2021.

Lee, J., Rollins, J. B., Spivey, J. P. Pressure transient testing. Texas, USA, Society of Petroleum Engineers, 2003.

Lu, J., Owayed, J. F., Xu, J., et al. An analytical model on production performance of multiple wells producing at constant bottomhole pressures. Special Topics and Reviews in Porous Media: An International Journal, 2019, 10(1): 31-48.

Lu, J., Shi, S. S., Rahman, M. M. New mathematical models for production performance of a well producing at constant bottomhole pressure. Special Topics and Reviews in Porous Media: An International Journal, 2018, 9(3): 261-278.

Lu, J., Ghedan, S., Tiab, D. Productivity equations for a multiple-well system in circular and rectangular reservoirs. Special Topics and Reviews in Porous Media: An International Journal, 2012, 3(4): 297-306.

Moore, T. V., Schilthuis, R. J., Hurst, W. The determination of permeability from field data. American Petroleum Institute Bulletin, 1933, 211(4).

Marhaendrajana, T., Blasingame, T. A. Decline curve analysis using type curves-evaluation of well performance behavior in a multiwell reservoir system. Paper SPE 71517 Presented at Annual Technical Conference and Exhibition, New Orleans, Louisiana, September 30-October 3, 2001.

Myint-U, T., Debnath, L. Green's functions and boundary-value problems. Linear Partial Differential Equations for Scientists and Engineers, 2007, 407-437.

Palacio, J. C., Blasingame, T. A. Decline-curve analysis using type curves-analysis of gas well production data. Paper SPE 25909 Presented at Rocky Mountain Regional Meeting, Denver, Colorado, USA, 12-14 April, 1993.

Stehfest, H. Algorithm 368: Numerical inversion of Laplace transforms. Communications of the ACM, 1970, 13(1): 47-49.

Tuma, J. J. Engineering mathematics handbook. Technometrics, 1971, 13(3).

Umnuayponwiwat, S., Ozkan, E., Raghavan, R. Pressure tran-

sient behavior and inflow performance of multiple wells in closed systems. Paper SPE 62988 Presented at Annual Technical Conference and Exhibition, Dallas, Texas, 1-4 October, 2000.

Valko, P. P., Doublet, L. E., Blasingame, T. A. Development and application of the Multiwell Productivity Index (MPI). SPE Journal, 2000, 5(1): 21-31.

Yang, Z. Analysis of production decline in waterflood reservoirs. Paper SPE 124613 Presented at Annual Technical Conference and Exhibition, New Orleans, Louisiana, 4-7 October, 2009.

Zakian, V. Numerical inversion of Laplace transform. Electronics Letters, 1969, 5(6): 120-121.

Zwillinger, D. CRC standard mathematical tables and formulae. CRC Press Taylor and Francis Group, New York City, USA, 1996.